

Supplementary Materials to:

Thermodynamics, Kinetics and Dilational Visco-elasticity of Adsorbed C_nEO_m Layers at the Aqueous Solution/Air Interface

Valentin B. Fainerman ¹, Volodymyr I. Kovalchuk ², Eugene V. Aksenenko ^{3,*},
Francesca Ravera ⁴, Libero Liggieri ⁴, Giuseppe Loglio ⁴, Alexander V. Makievski ¹,
Emanuel Schneck ⁵ and Reinhard Miller ^{5,*}

¹ SINTERFACE Technologies, Berlin D12489, Germany; fainerman@ukr.net (V.B.F.); a.makievski@sinterface.com (A.V.M.)

² Institute of Biocolloid Chemistry, National Academy of Sciences of Ukraine, Kyiv (Kiev) 03680, Ukraine; vladim@koyal.kiev.ua

³ Institute of Colloid Chemistry and Chemistry of Water, National Academy of Sciences of Ukraine, Kyiv (Kiev) 03680, Ukraine; Eugene_Aksenenko@ukr.net

⁴ CNR-Institute of Condensed Matter Chemistry and Technologies for Energy, Unit of Genoa, 16149 Genoa, Italy; francesca.ravera@ge.icmate.cnr.it (F.R.); libero.liggieri@ge.icmate.cnr.it (L.L.); giuseppe.loglio@ge.icmate.cnr.it (G.L.)

⁵ Physics Department, Technical University Darmstadt, 64289 Darmstadt, Germany; schneck@fkp.tu-darmstadt.de

* Correspondence: miller@fkp.tu-darmstadt.de, Eugene_Aksenenko@ukr.net

Received: date; Accepted: date; Published: date

S1. Calculation details and software outlook

It is preferable to perform the calculations using the model variables converted into the dimensionless form. Introducing the quantities:

$$p = \Pi\omega_{10}/RT, \quad \kappa = \varepsilon RT/\omega_{10}, \quad (\text{S.1 a,b})$$

$$\Omega = \omega/\omega_{10}, \quad \Omega_1 = \omega_1/\omega_{10} = 1 - \kappa p \theta, \quad \Omega_2 = \omega_2/\omega_{10}, \quad (\text{S.2 a,b,c})$$

one transforms the equation of state, Eq. (2) and adsorption isotherm, Eq. (3) into:

$$p = -\left[\ln(1-\theta) + \theta(1-1/\Omega) + a\theta^2 \right], \quad (\text{S.3})$$

$$bc = \frac{\Omega_2 - \Omega}{\Omega_2 - \Omega_1} \frac{\theta}{\Omega} (1-\theta)^{-\Omega_1} \exp(-2a\theta\Omega_1), \quad (\text{S.4})$$

respectively, and Eq. (7) becomes:

$$\frac{\Omega - \Omega_1}{\Omega_2 - \Omega} = \left(\frac{\Omega_2}{\Omega_1} \right)^\alpha (1-\theta)^{\Omega_2 - \Omega_1} \exp[(\Omega_2 - \Omega_1) \cdot (2a\theta)]. \quad (\text{S.5})$$

It could be seen that Eqs. (S.4) and (S.5), with the value of Ω_1 expressed in terms of θ and Ω via the relation Eq. (S.2 b) and (S.3), constitute the set from which the model variables θ and Ω could be calculated as functions of the surfactant concentration c for any non-contradictory set of model parameters $b = b_1$, ω_{10} , ω_2 , a , α and ε . With these variables, the values of Π (hence the surface tension γ), total adsorption $\Gamma = \theta/\omega = \theta/(\Omega \cdot \omega_{10})$, and partial adsorptions $\Gamma_1 = \Gamma \cdot (\Omega_2 - \Omega)/(\Omega_2 - \Omega_1)$, $\Gamma_2 = \Gamma \cdot (\Omega - \Omega_1)/(\Omega_2 - \Omega_1)$ could be calculated.

To solve the set of equations described above, the Newton-Raphson algorithm as described in [S.1] was applied. For the chosen set of model parameters, the isotherm was tabulated along the

concentration axis with nodes distributed in the logarithmic scale, starting from the c values sufficiently small for the initial approximations $\theta \cong c \cdot b$, $\Omega \cong \Omega_2$ to be valid; at each subsequent step the initial approximation was calculated via suitable extrapolation formulae.

The model was implemented as a module integrated into the computer program IsoPlotM, employed also for calculations described earlier. The program possesses the graphic interface shown in Fig. S.1, and is capable to perform the calculations of tensiometric and rheological quantities which are displayed on the screen and stored in files compatible for treating by common matrix processing packages (e. g. Excel or Origin). The software is under development for routine application by many external users.

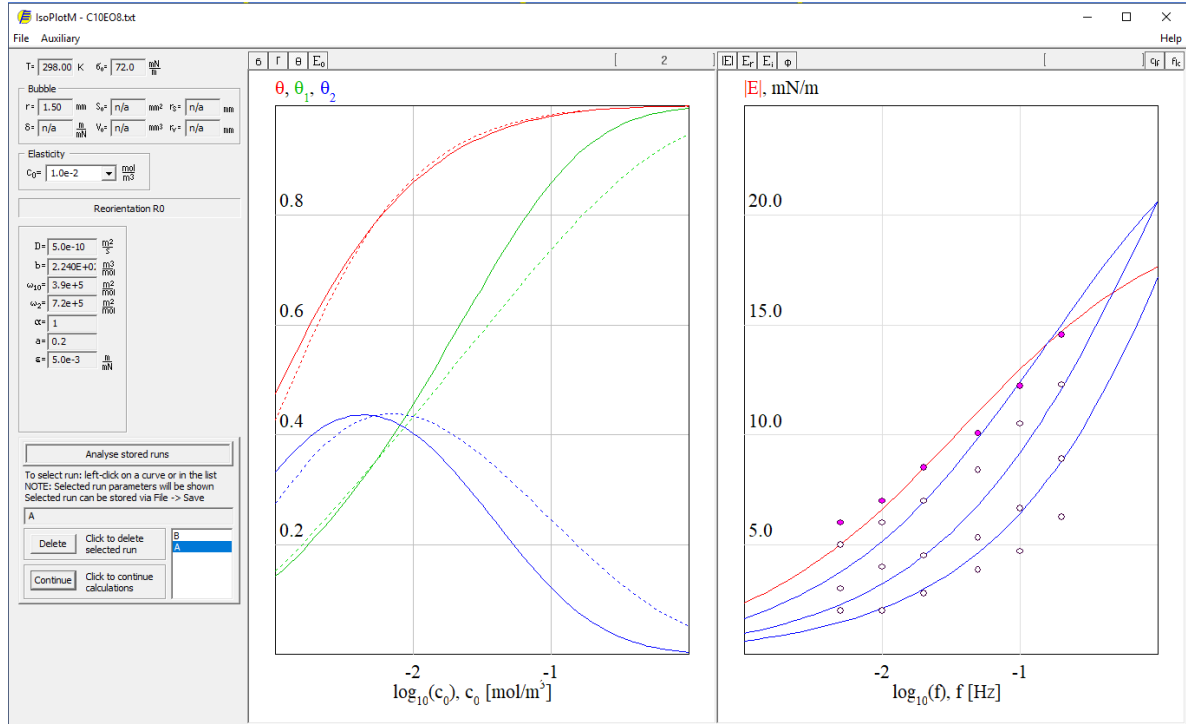


Figure S1. The interface of the computer program IsoPlotM used to perform the model calculations described in the article. From left to right: the **Control Panel**, the **Tensiometry Window** to display the dependencies of model variables on the surfactant bulk concentration, and the **Rheology Window** to display the dependencies of visco-elastic values on the concentration or surface area oscillation frequency.

S2. Response of calculated values to the variation of model parameters

To analyse the effect caused by the variation of model parameters onto the calculated dependencies, it should be noted first that the model essentially assumes that the adsorbed layer is subdivided into two subsystems, each consisting of the molecules which exist either in state 1, or in state 2. This implies the subdivision of the total coverage θ into two terms, see Eq. (5):

$$\theta = \omega\Gamma = \theta_1 + \theta_2 = \omega_1\Gamma_1 + \omega_2\Gamma_2, \quad (\text{S.6})$$

This is illustrated in Fig. S1 above, where the partial coverages θ_1 and θ_2 are shown in the Tensiometry Window by green and blue curves, respectively. In this window, the results of actual calculations for C₁₀EO₈ with the parameters shown in Table 1 are displayed by solid lines; the dashed lines correspond to the same parameter set except for $\omega_{10} = 4.9 \times 10^5 \text{ m}^2/\text{mol}$, while the Rheology Window shows the dependencies of $|E|$ on surface area oscillation frequency f at various surfactant concentrations c_0 . The plots of the coverages could be compared to those of adsorbed amounts, Fig. 6; note however that the value of Γ_1 is proportional to the θ_1 value via the coefficient ω_1 which depends on the surface pressure Π and total surface coverage θ , see Eq. (S.2 b) above.

Therefore, the response of the observable values, which in the present case are the surface tension and visco-elasticity modulus, to the variation of model parameters could be considered via the response of the coverages, which obviously govern the behaviour of the system. In particular, it is seen from Fig. S1 above that the coverage θ_2 (by molecules in the state with larger molar area) is more significant in the intermediate concentration range, while in the higher concentration range the θ_1 value plays the major role.

The response of the quantities θ_1 and θ_2 to the variations of model parameters is illustrated by Figures S2 to S6. In these Figures the solid curves show the dependencies of θ_1 and θ_2 on the C₁₀EO₈ surfactant concentrations calculated with the parameters listed in Table 1. The dash-dotted curves correspond to the dependencies changed in response to an increase of certain parameter as indicated in the respective Figure. As can be expected, the decrease of a parameter results in opposite trend of the analysed coverage.

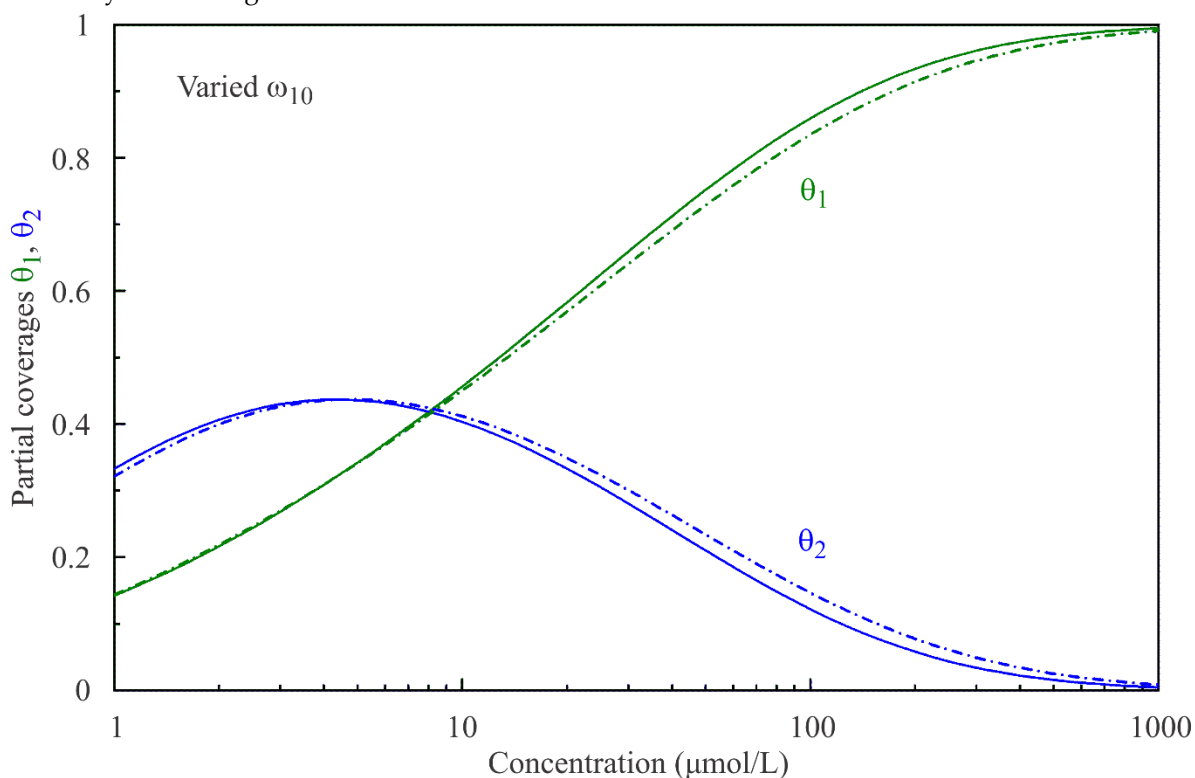


Figure S2. The response of the coverages to positive deviation of ω_{10} by $0.2 \times 10^5 \text{ m}^2/\text{mol}$.

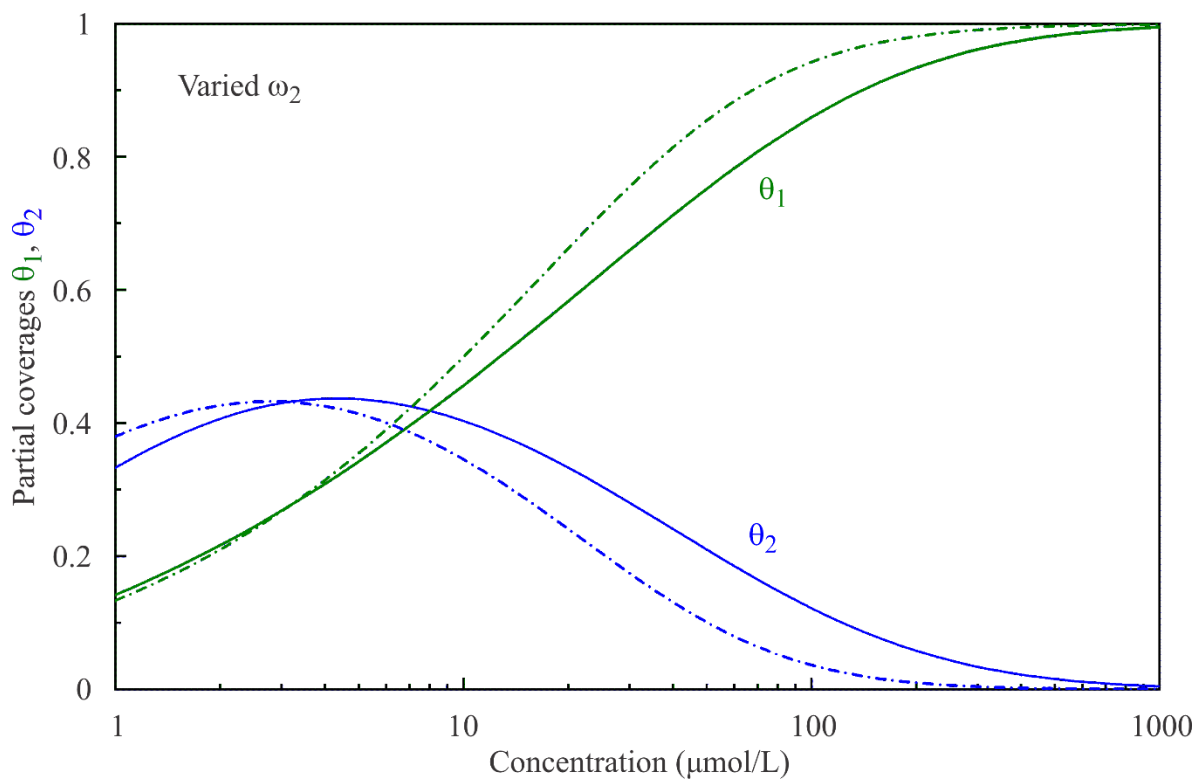


Figure S3. The response of the coverages to positive deviation of ω_2 by $2.2 \times 10^5 \text{ m}^2/\text{mol}$.

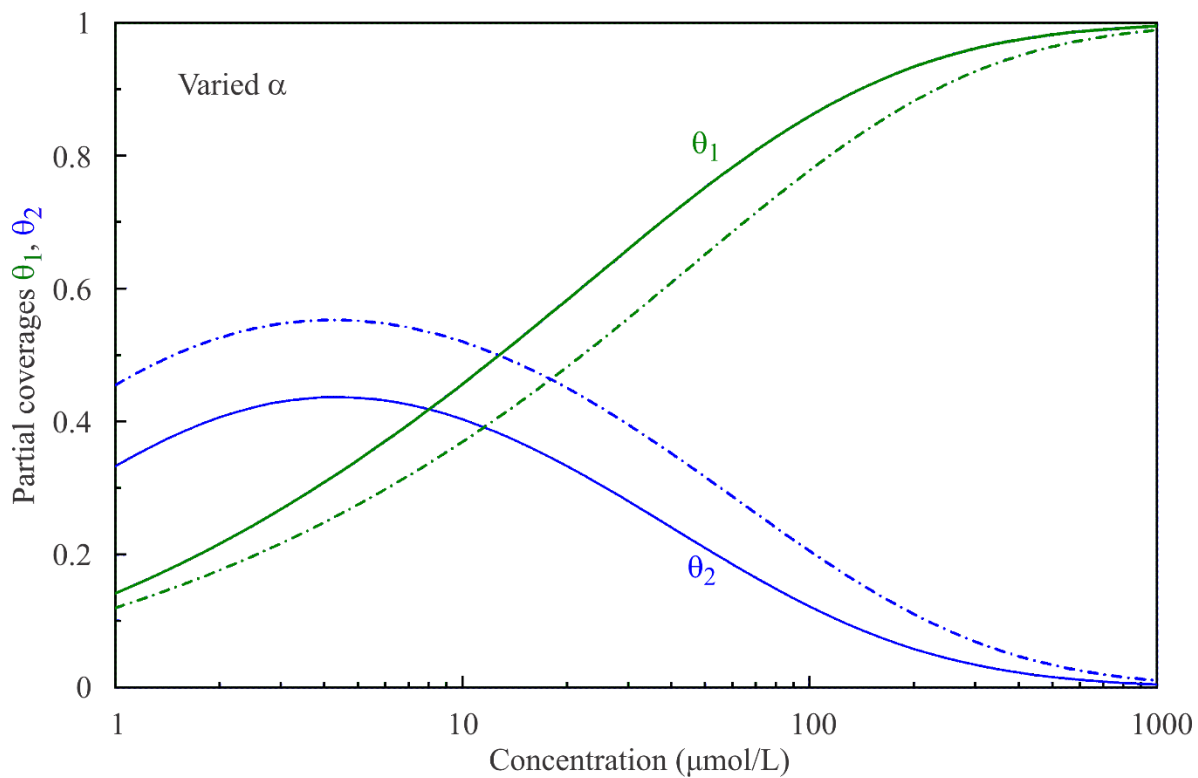


Figure S4. The response of the coverages to positive deviation of α by 1.

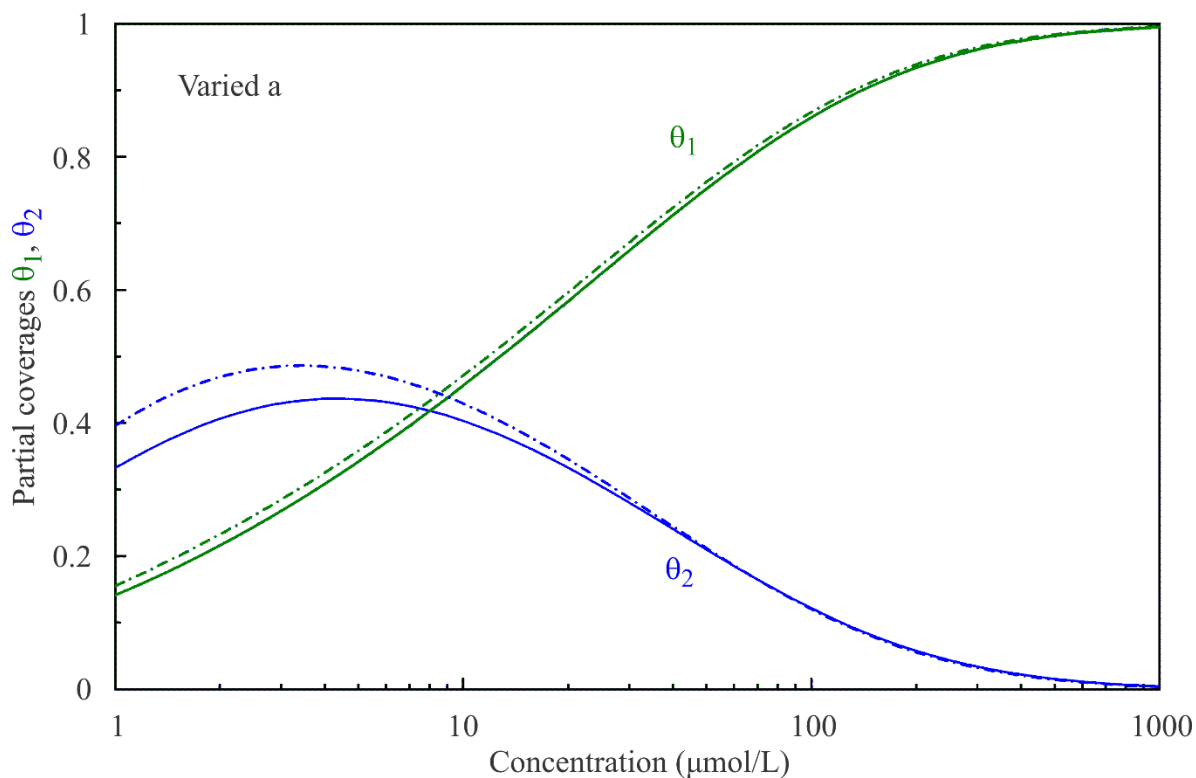


Figure S5. The response of the coverages to positive deviation of a by 0.2.

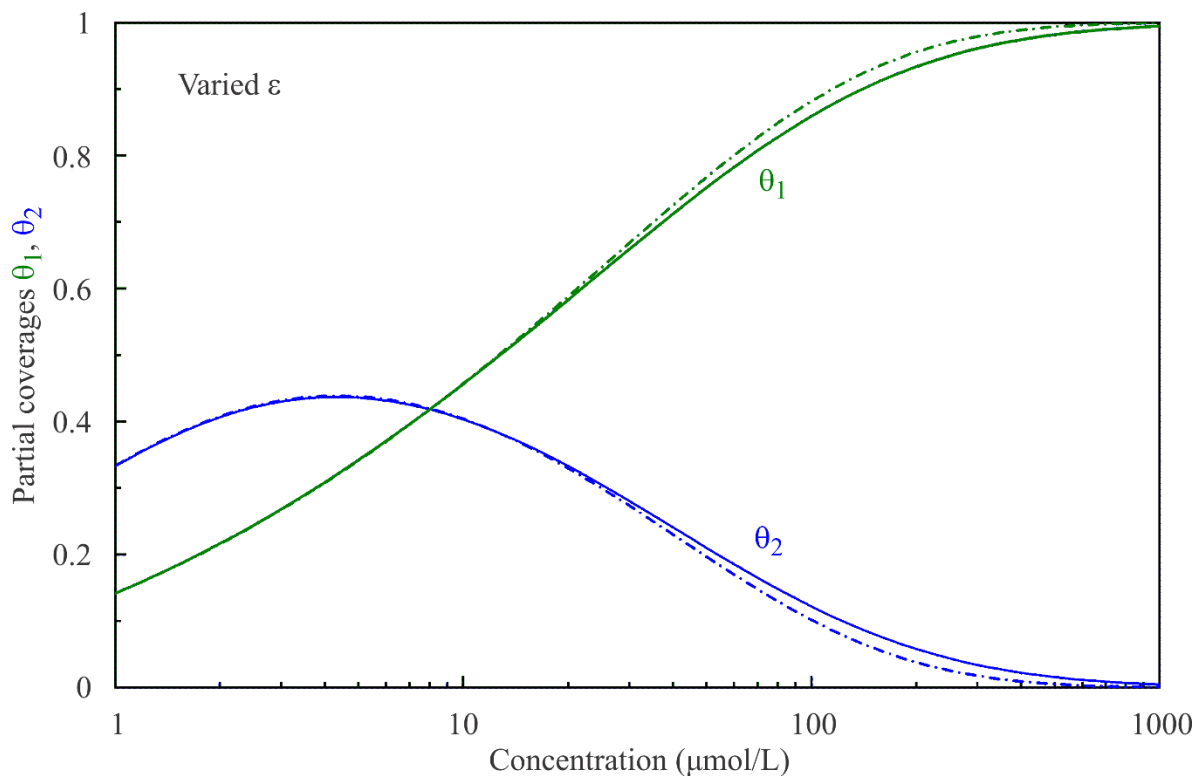


Figure S6. The response of the coverages to positive deviation of ϵ by 0.002 m/mN.

It is seen from Fig. S2 that the increase of ω_{10} leads to the decrease of the corresponding coverage θ_1 in the high concentration range, because this makes the surface less available for molecules in state 1; this also 'shifts the balance' between the states 1 and 2 resulting in the increase of the number of molecules available for the partial coverage in state 2. In a quite similar way, the increase of ω_2 shifts

the maximum of surface coverage by molecules in state 2 towards lower surfactant concentrations as shown in Fig. S3, because it makes the adsorption of these molecules less preferable at higher concentrations. Figure S4 demonstrates the fact that, as shown by Eq. (6), the increase of α leads to the increase of the surface activity (and hence the adsorption) of the surfactant in state 2. The increase of the parameter a , as shown in Fig. S5, corresponds to the increase of attractive interactions between the adsorbed molecules; this factor is of significance in the lower concentration range, while at high concentrations the steric factor becomes prevalent, note the logarithmic term in the equation of state, Eq. (S.3). Finally, the increase of ε results in the decrease of ω_1 , which can be seen by comparing Fig. S2 and Fig. S6; however, these factors do not mimic each other because the relation Eq. (S.2) involves additional dependencies of ω_1 on the surface pressure and total coverage.

The influence of model parameters on the observable quantities, namely the surface tension and the visco-elasticity modulus, could be discussed basing on the considerations presented above, keeping in mind that this influence involves the contributions of both coverages simultaneously. The response of these quantities to the variation of model parameters is represented in Figures S7 – S12, where experimental values are represented by symbols. Note that, in line with the data and discussion in the main text of the article, each figure shows the dependence of surface tension on the concentration (left ordinate vs bottom abscissa axes) and the dependence of visco-elasticity modulus on frequency (right ordinate vs top abscissa axes) for two different $C_{10}EO_8$ surfactant concentrations, 10 and 100 $\mu\text{mol/L}$. It is essential that the parameter $b = b_1$ enters the equations only in the product $b \cdot c$, see adsorption isotherm equation, Eq. (S.4) above, and thus should be considered as the concentration-scaling factor.

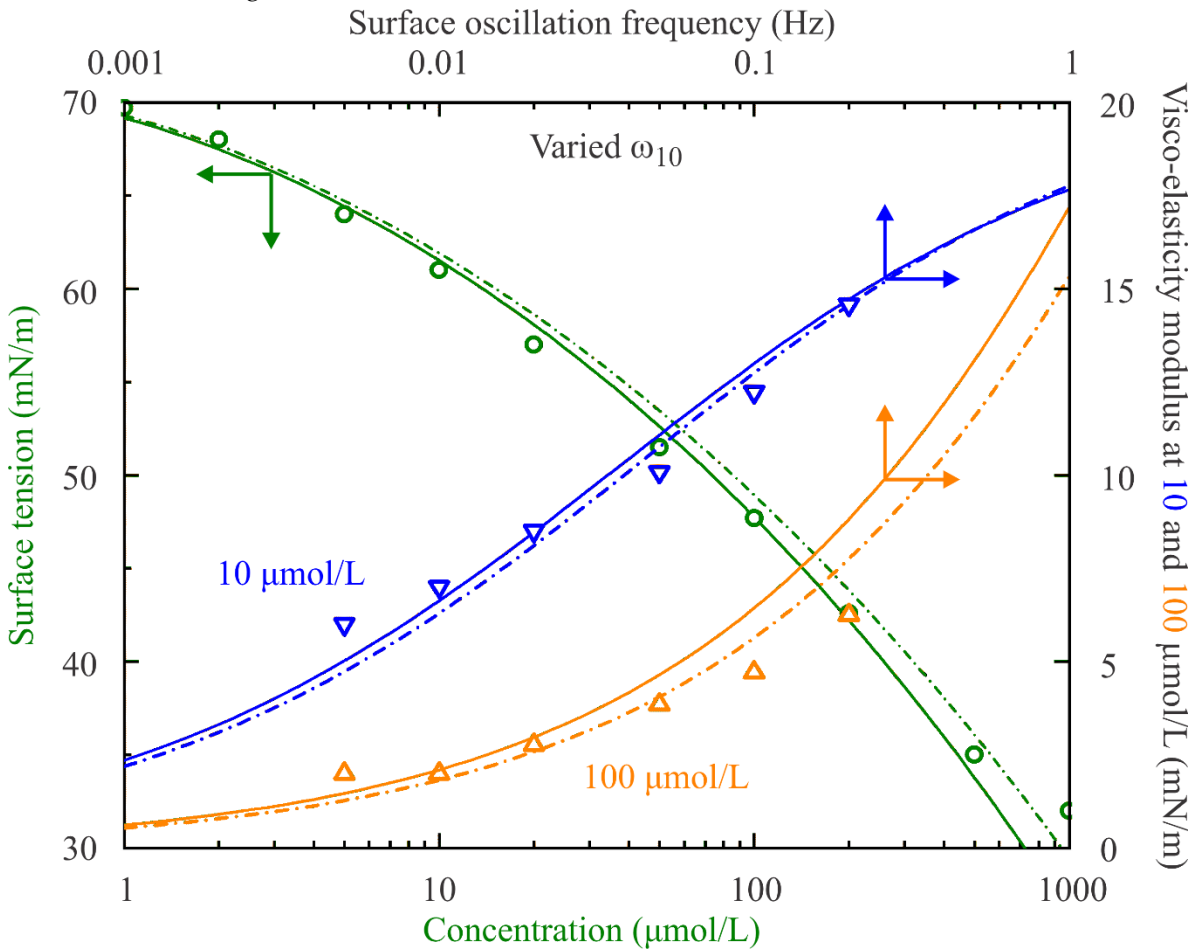


Figure S7. The response of the observables to positive deviation of ω_{10} by $0.2 \times 10^5 \text{ m}^2/\text{mol}$.

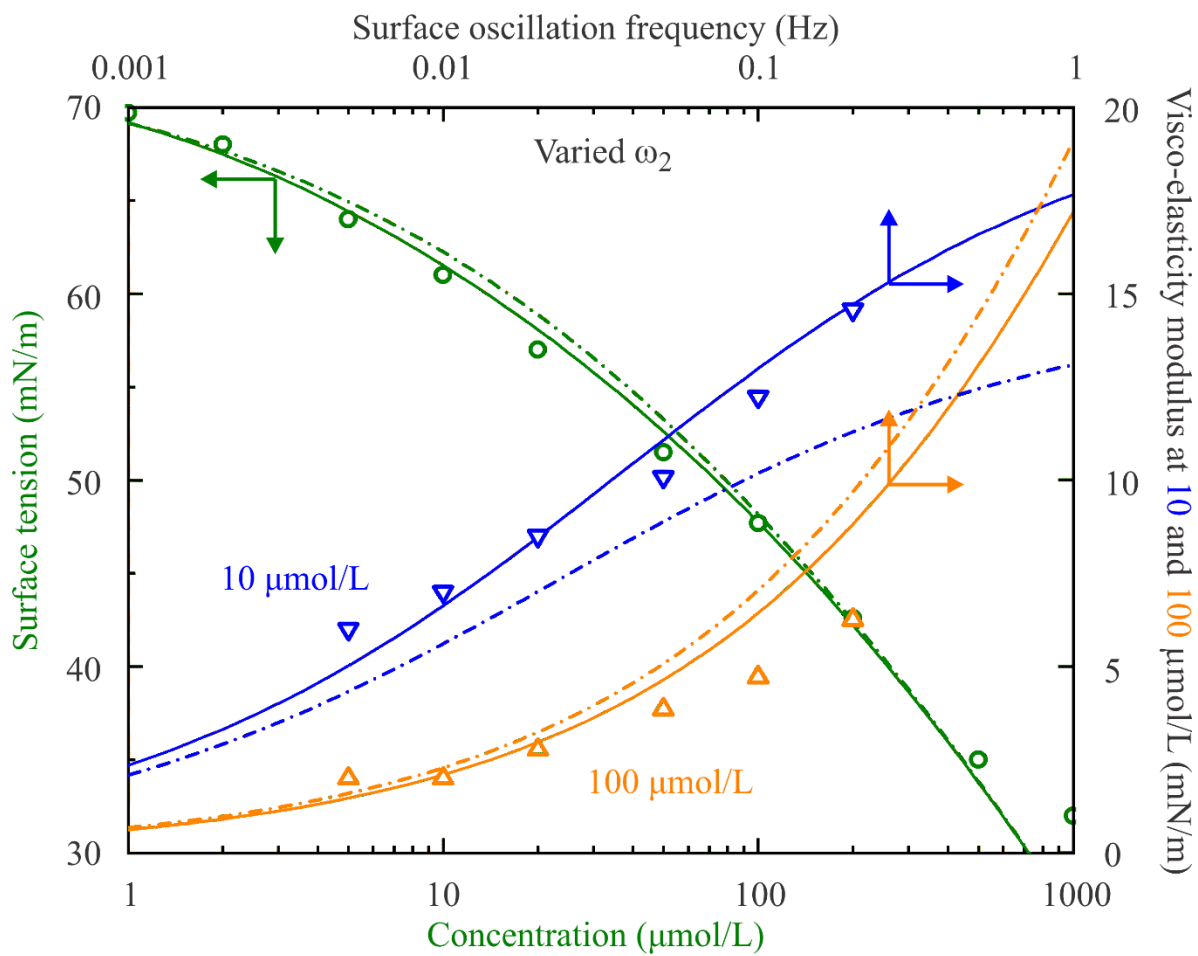


Figure S8. The response of the observables to positive deviation of ω_2 by $2.2 \times 10^5 \text{ m}^2/\text{mol}$.

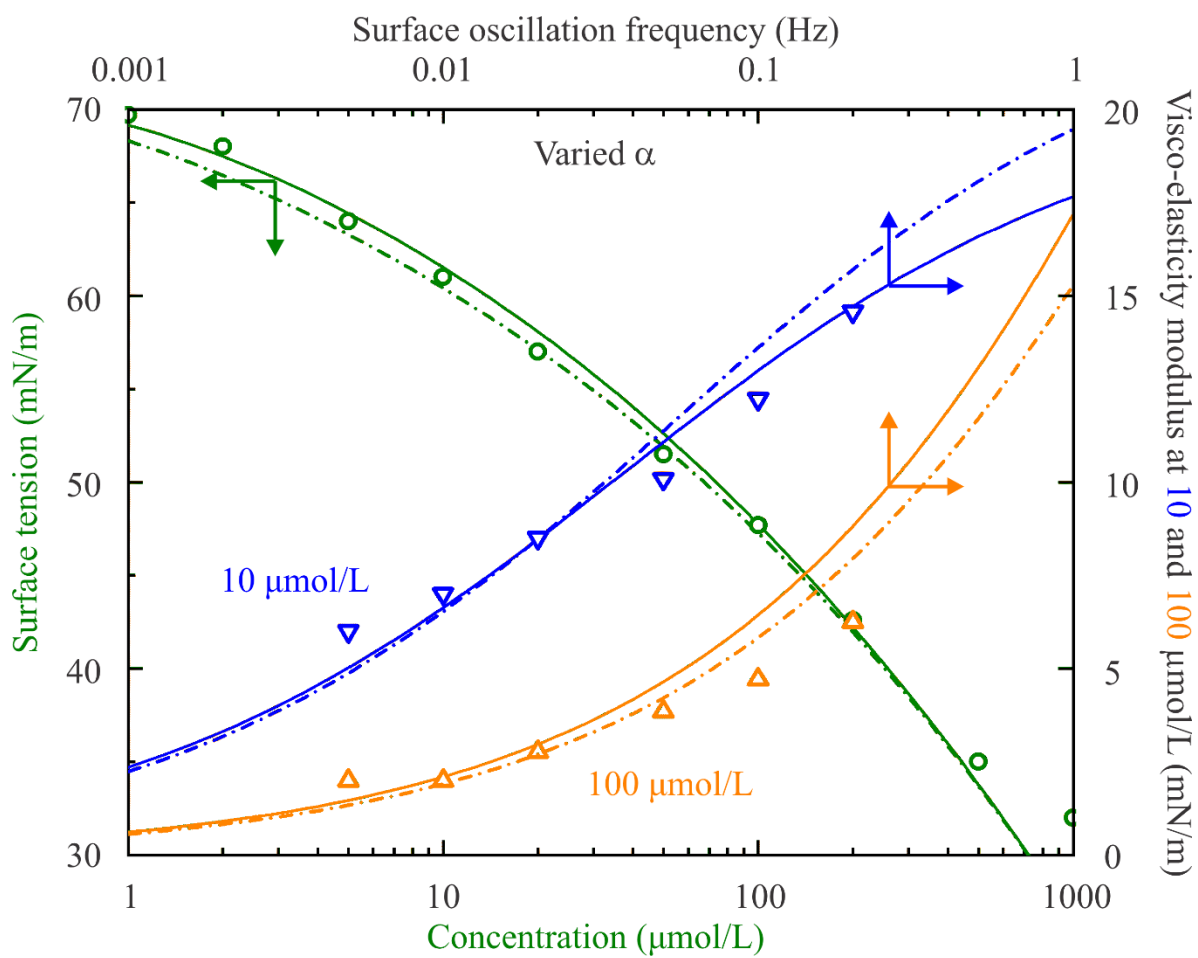


Figure S9. The response of the observables to positive deviation of α by 1.

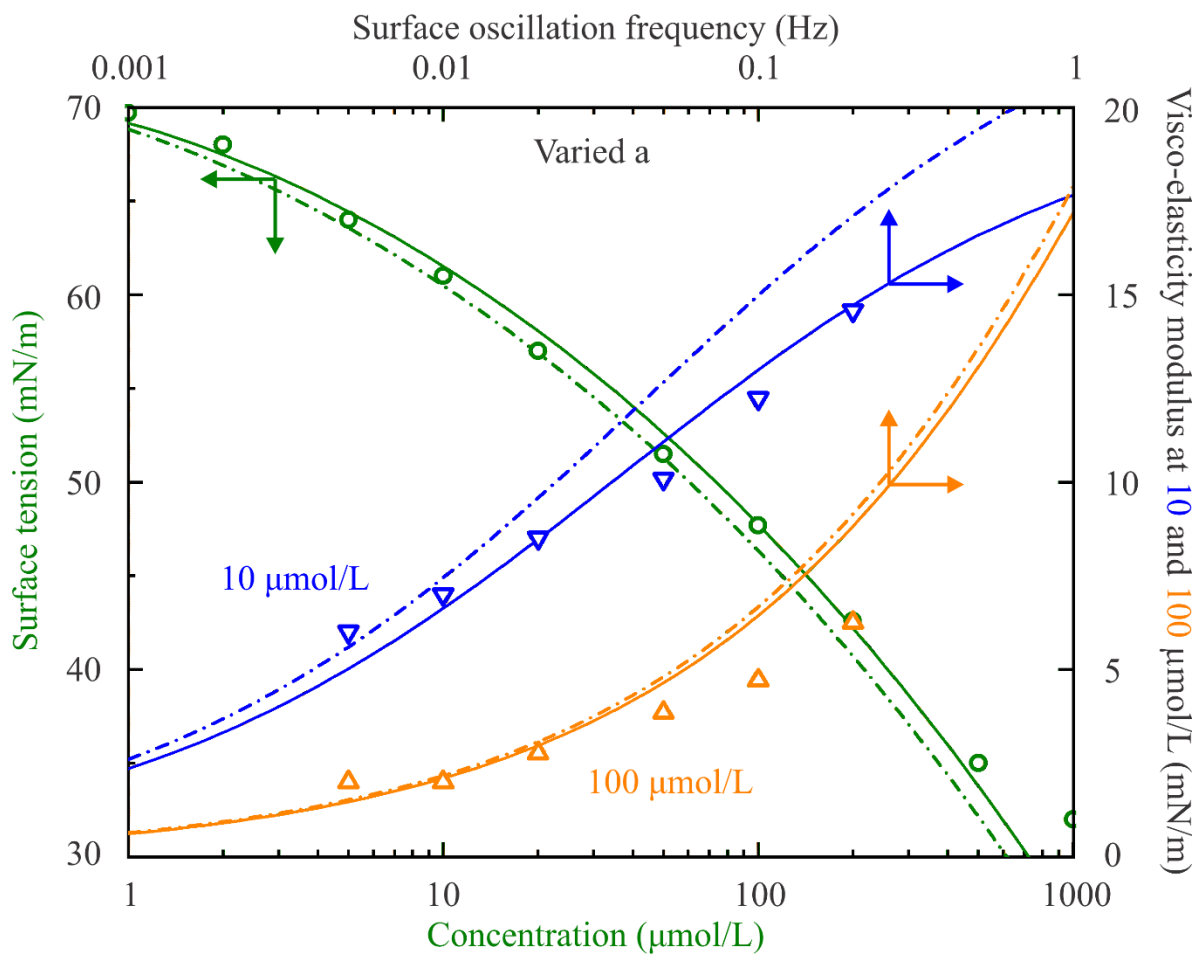


Figure S10. The response of the observables to positive deviation of a by 0.2.

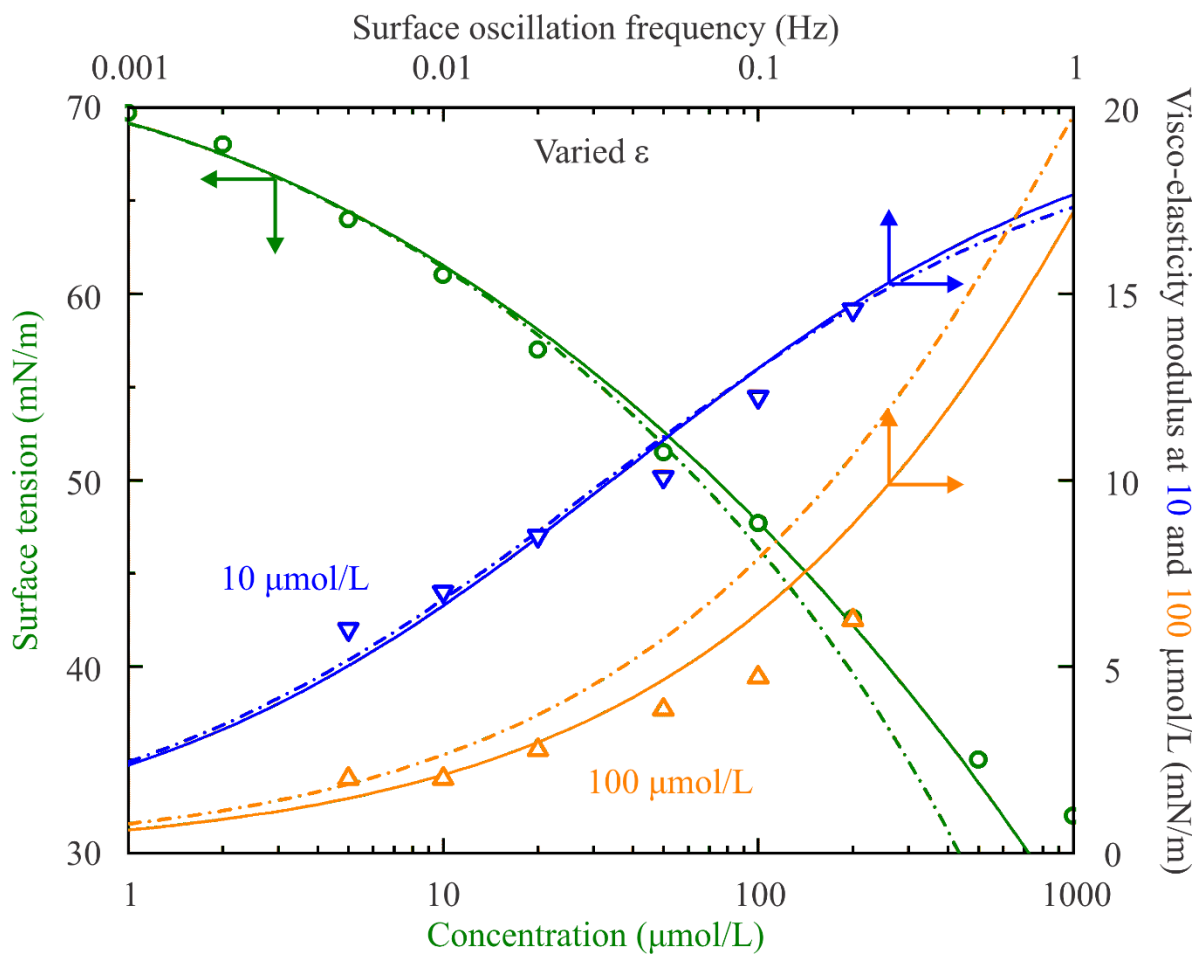


Figure S11. The response of the observables to positive deviation of ϵ by 0.002 m/mN.

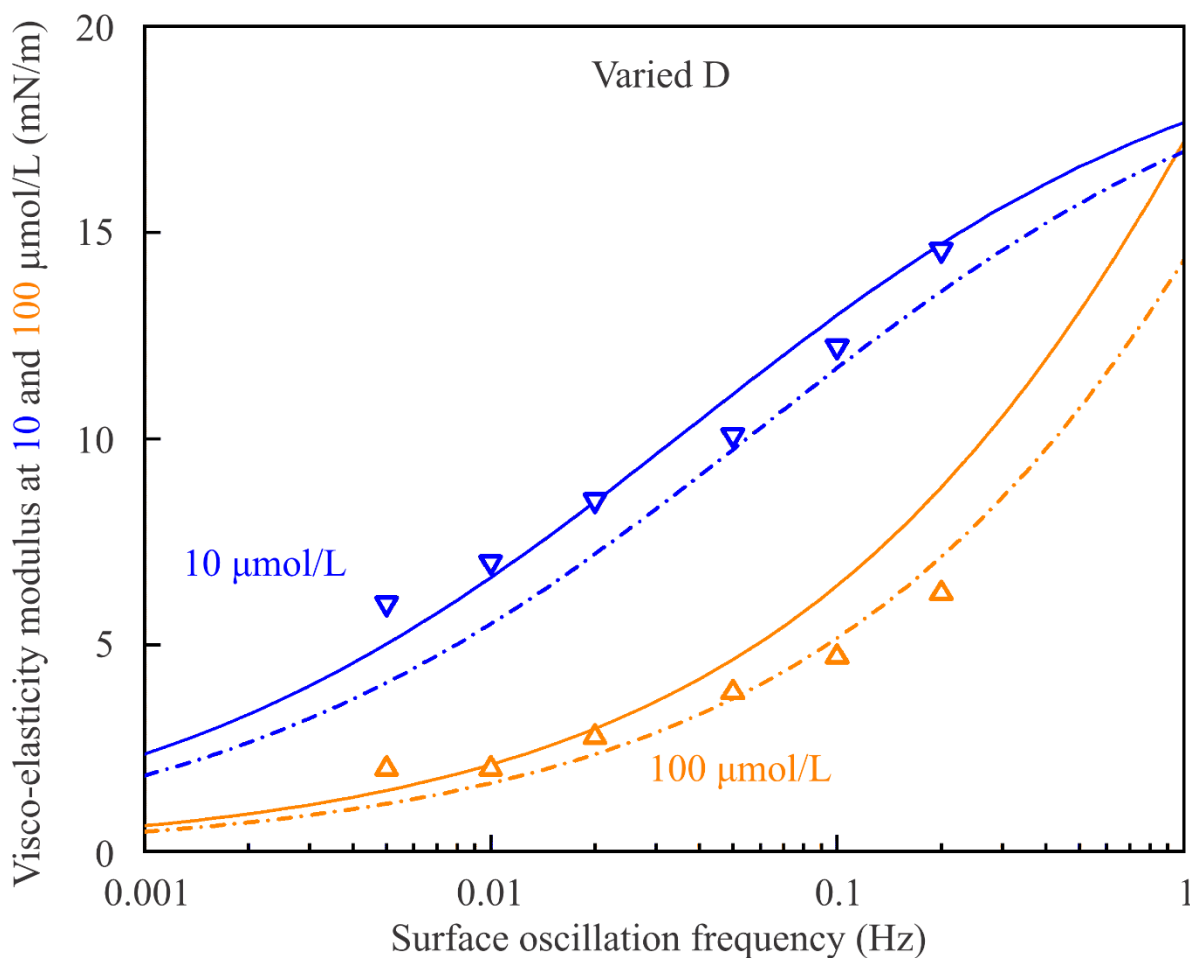


Figure S12. The response of the visco-elasticity modulus to positive deviation of D by $3.0 \times 10^{-10} \text{ m}^2/\text{s}$.

It is seen from Fig. S7 that the increase of ω_{10} quite expectably leads to the increase of the surface tension, as larger molecular area reduces the number of molecules capable for the adsorption at the interface. This effect is more essential in the high concentration range (where the majority of molecules exist in state 1), which explains also the fact that the effect caused by the variation of this parameter on the visco-elasticity modulus is more noticeable for the module dependence on frequency at higher surfactant concentration, cf. the dependencies for 10 and 100 $\mu\text{mol/L}$ in this Figure. In a quite similar way, it could be seen from Fig. S8 that the variation of ω_2 leads to the variations of observable values in an intermediate concentration range, where the surface coverage by the molecules in state 2 exhibits a maximum. Similar considerations also apply to the dependencies shown in Fig. S9, which reflects the fact already mentioned regarding Fig. S4, namely the increase of the ratio of surface activity coefficients b_2/b_1 with the increase of the α value, which leads to the decrease of surface tension mainly at low surfactant concentrations. Also Fig. S10 is explainable noting that the increase of a leads to the increase of intermolecular attraction which in turn decreases the surface tension. This effect affects the viscoelasticity modulus mostly at low surfactant concentrations, in line with the discussion regarding Fig. S5 above.

Figure S11, similarly to Fig. S6 above, shows that the influence of the variation of the intrinsic compressibility ε affects the behaviour of observables mostly in the high concentration range, because it is the domain where the ω_1 value is varied according to Eq. (S.2). Finally, the variation of the diffusion coefficient D affects the visco-elasticity modulus only; it could be seen from Eq. (8) that the increase of D results in the decrease of the modulus, which is shown in Fig. S12.

Reference

1. Press, W.H.; Teukolsky, S.A.; Vetterling, W.T.; Flannery, B.P. *Numerical Recipes in C*. Cambridge University Press, 1999.